

DEK Is a Poly(ADP-Ribose) Acceptor in Apoptosis and Mediates Resistance to Genotoxic Stress^{∇†}

F. Kappes,^{1,2} J. Fahrner,¹ M. S. Khodadoust,^{2,3} A. Tabbert,¹ C. Strasser,¹ N. Mor-Vaknin,^{2,3}
M. Moreno-Villanueva,¹ A. Bürkle,¹ D. M. Markovitz,^{2,3,4} and E. Ferrando-May^{1*}

University of Konstanz, Department of Biology, Box X911, D-78457 Konstanz, Germany,¹ and Department of Internal Medicine, Division of Infectious Diseases,² Program in Immunology,³ and Cellular and Molecular Biology Program,⁴ University of Michigan Medical Center, Ann Arbor, Michigan 48109

Received 24 October 2007/Returned for modification 8 January 2008/Accepted 4 March 2008

DEK is a nuclear phosphoprotein implicated in oncogenesis and autoimmunity and a major component of metazoan chromatin. The intracellular cues that control the binding of DEK to DNA and its pleiotropic functions in DNA- and RNA-dependent processes have remained mainly elusive so far. Our recent finding that the phosphorylation status of DEK is altered during death receptor-mediated apoptosis suggested a potential involvement of DEK in stress signaling. In this study, we show that in cells committed to die, a portion of the cellular DEK pool is extensively posttranslationally modified by phosphorylation and poly(ADP-ribosylation). Through interference with DEK expression, we further show that DEK promotes the repair of DNA lesions and protects cells from genotoxic agents that typically trigger poly(ADP-ribose) polymerase activation. The posttranslational modification of DEK during apoptosis is accompanied by the removal of the protein from chromatin and its release into the extracellular space. Released modified DEK is recognized by autoantibodies present in the synovial fluids of patients affected by juvenile rheumatoid arthritis/juvenile idiopathic arthritis. These findings point to a crucial role of poly(ADP-ribosylation) in shaping DEK's autoantigenic properties and in its function as a promoter of cell survival.

Human DEK is an abundant and highly conserved nuclear protein that has long been implicated in carcinogenesis and autoimmune disorders (for a review, see references 50 and 60). Originally isolated from a specific subtype of acute myeloid leukemia (55), the gene encoding DEK is expressed under the control of transcription factors E2F and YY1 (10, 49). High levels of DEK support cell immortalization and inhibit both senescence and apoptosis, as shown in cells infected with high-risk human papillomavirus E7 (1, 62, 63). DEK is also upregulated in a variety of aggressive human tumors, including retinoblastoma, colon and bladder cancer, and melanoma (e.g., see references 10, 19, 28, 30, and 37).

In the nucleus, DEK is involved in a variety of DNA- and RNA-dependent processes, such as DNA replication (2), splice site recognition (51), and gene transcription. Here it can function as either an activator (9) or a repressor (16, 20, 45). The diversity of these effects is in line with DEK's described function as a possible regulator of chromatin architecture, which may affect genome activity at various levels in a highly context-dependent manner. In fact, DEK has been shown *in vitro* to be a modifier of DNA higher-order structure, acting in concert with topoisomerase I to introduce constrained positive supercoils in closed circular DNA plasmids and simian virus 40 (SV40) minichromosomes (24, 25, 58, 59). Accordingly, DEK was shown to bind to DNA in a structure-specific rather than

sequence-specific manner and to reduce the accessibility of chromatin to components of the replication machinery (2, 58). Beyond its effects on DNA topology, DEK can modulate the activity of other chromatin-associated proteins, such as P/CAF and p300/CBP (27), the p65 subunit of NF- κ B (45), and the transcription factor AP2- α (9), as well as the nuclear splicing factor U2AF (51).

Posttranslational modifications play an important role in regulating DEK's binding to DNA and chromatin proteins: acetylation and phosphorylation decrease DEK's affinity for DNA (11, 24), while the interaction of DEK with U2AF requires phosphorylation (51). How the posttranslational modification of DEK is regulated *in vivo*, however, is largely unclear. We recently observed a pronounced reduction in the phosphorylation level of DEK in cells undergoing cell death by apoptosis (53).

Another posttranslational modification of DEK was identified in an *in vitro* transcription system derived from human nuclear extracts. Here, poly(ADP-ribosylation) of DEK by poly(ADP-ribose) polymerase 1 (PARP1) was required to displace DEK from a chromatin substrate and allow access of transcription factors (17). The poly(ADP-ribosylation) of nuclear proteins by PARP1 is implicated in many aspects of genomic activity that require remodeling of local chromatin architecture, in particular, the repair of DNA lesions by the base excision repair pathway (reviewed in references 8 and 47). The occurrence and significance of a potential PARP1-DEK interaction has not been investigated *in vivo* so far and could contribute to understanding the mechanisms underlying DEK's function in oncogenesis.

In addition, the observation that DEK is a substrate for poly(ADP-ribosylation), resulting in the dissociation of DEK

* Corresponding author. Mailing address: University of Konstanz, Department of Biology, Box X911, D-78457 Konstanz, Germany. Phone: 49-7531-884054. Fax: 49-7531-884033. E-mail: elisa.may@uni-konstanz.de.

† Supplemental material for this article may be found at <http://mcb.asm.org/>.

[∇] Published ahead of print on 10 March 2008.

from DNA, suggests that under conditions of sustained PARP1 activation, DEK may be displaced from chromatin and eventually released from the nuclear compartment. This putative scenario could have important implications for the role of DEK in the pathogenesis of autoimmunity, another disease besides cancer in which DEK is crucially involved. Circulating anti-DEK autoantibodies are found in different autoimmune disorders, including systemic lupus erythematosus and sarcoidosis (14). High concentrations of DEK are also present in synovial fluids from patients affected by juvenile rheumatoid arthritis/juvenile idiopathic arthritis (JRA/JIA) (35). Prompted by our proteome analysis that highlighted a change in the phosphorylation status of DEK in dying cells (53), we hypothesized that apoptosis could provide an attractive *in vivo* setting for the study of DEK's posttranslational modifications. Our results show that a fraction of DEK is heavily modified by phosphorylation and poly(ADP-ribose)ation in dying cells. These DEK species are efficiently released from chromatin and eventually from the cell, providing a further mechanism by which DEK can be presented to the immune system. Further, we demonstrate that DEK is involved in the repair of DNA strand breaks, thus supporting a role for DEK in the poly-(ADP-ribose)-dependent (PAR-dependent) maintenance of genomic integrity.

MATERIALS AND METHODS

Antibodies. For the detection of DEK, either a mouse monoclonal antibody (clone 2; BD Biosciences) or an affinity-purified polyclonal antibody (24) was used. Anti-phosphoserine H2AX antibodies (clone JBW301) were obtained from Upstate. HMG1-specific polyclonal antibodies were from Abcam (catalog no. ab18256), HMG2-specific polyclonal antibodies were from BD Biosciences, and anti-active caspase-3 antibodies were from Cell Signaling.

Mouse monoclonal antibodies recognizing PAR were immunopurified on a protein A column (Sigma) from 10H hybridoma cell culture supernatant (kind gift of M. Miwa and T. Sugimura) (26). Mouse monoclonal antibodies directed against PARP1 were harvested from the culture supernatant of CII10 hybridoma cells (kind gift of G. G. Poirier).

DEK-specific autoantibodies were purified from the synovial fluid of one patient with a positive antinuclear antibody status (kind gift of David Glass, Cincinnati Children's Hospital Medical Center, Cincinnati, OH).

Cell culture procedures. Jurkat cells were grown in RPMI 1640 medium (Invitrogen) supplemented with 10% fetal calf serum (FCS), 100 U/ml penicillin-streptomycin. HeLa, the Phoenix amphotropic retroviral packaging cell line, and the lentiviral packaging cell line HEK 293 FT were grown in Dulbecco's modified Eagle's medium (Invitrogen) supplemented with 10% FCS, 100 U/ml penicillin-streptomycin. All cultures were maintained in a humidified atmosphere at 37°C and 5% CO₂.

For *in vivo* labeling with [³²P]orthophosphate, Jurkat cells were washed three times with phosphate- and serum-free RPMI medium and then cultivated in phosphate- and serum-free medium supplemented with 40 mCi/ml of ³²Pi (carrier free; ICN) for the indicated time.

For the generation of a Jurkat cell line stably expressing a dominant-negative mutant of ICAD (43), the retroviral expression vector pBABE-ICAD-dm was used to transfect Phoenix cells to produce high-titer retrovirus for infection. Briefly, 5 × 10⁶ cells were seeded in a 10-cm petri dish 24 h before being transfected with 20 μg pBABE-ICAD-dm or pBABE DNA (empty vector) by using calcium phosphate. The medium was replaced after 24 h. The virus-containing culture supernatant was harvested 48 h and 72 h after transfection and used immediately for the transduction of Jurkat cells. After filtration through a 0.45-μm filter and addition of 4 μg/ml Polybrene, the supernatant (at 48 h) was used to resuspend Jurkat cells at a density of 1 × 10⁵ cells/ml. The cell suspension was distributed in six-well plates and spin infected for 90 min at 32°C and 1,500 × g. After 5 h at 37°C, the medium was replaced. The cells were collected 16 h later, and the spin transduction procedure was repeated with supernatant (at 72 h). Cells were then collected and cultured for 2 weeks in the presence of 1.5 μg/ml puromycin. Resistant clones were isolated by dilution cloning in 96-well plates.

shRNA procedures. To achieve stable DEK knockdown in Jurkat and HeLa cells, third generation, self-inactivating lentiviral constructs were used. Two different systems were chosen for successful knockdown of DEK. For selection by enhanced green fluorescent protein (EGFP), three packaging vectors (pRSVrev, pMDLg/pRRE, and pHCMV-G, providing *rev*, *gag*, *pol*, and envelope protein G) and a control plasmid, H1-LV, producing no short hairpin RNA (shRNA) but producing EGFP as well as a double anti-DEK shRNA-producing construct (H1/U6LV_1450/960, targeting DEK mRNA at nucleotide positions 960 and 1450) were used. For puromycin selection, two plasmids from the Sigma Mission shRNA library, PLKO.1_DEK832 and PLKO.1_DEK1165 (targeting DEK mRNA at nucleotide positions 832 and 1165), were used to knock down DEK. As a control vector, PLKO.1_PURO, coding for the puromycin resistance gene and no shRNA, was used. Viruses produced by using these vectors are referred to as GFP-control, DEK-DL-LV, Puro-c, DEK-832, and DEK-1165.

A 4-day infection protocol was used for lentivirus production and infection of target cells. HEK 293 FT cells were seeded on 10-cm dishes on the first day to be 90% confluent at time of transfection. On the second day, HEK 293 FT cell culture medium was supplemented with 25 μg chloroquine prior to transfection with 4 μg of each individual plasmid using calcium chloride. Eight hours posttransfection, medium was replaced and virus-containing supernatant was harvested at 12, 24, and 36 h posttransfection. For the infection of target cells, virus-containing supernatant was filtered through 0.45-μm filters and supplemented with 4 μg/ml Polybrene prior to incubation. The infection of target cells was repeated twice for a total of 10 h. Selection by puromycin (2 μg/ml for Jurkat and 1 μg/ml for HeLa) was started 48 h postinfection for up to 10 days. For sorting by fluorescence-activated cell sorter analysis, cells were grown for 72 h and sorted by GFP gating. The sorted cells were 100% GFP positive and kept in culture for a maximum of five passages.

Preparation of cell extracts, immunoprecipitation, and immunoblot analysis. Jurkat cells were seeded in dishes of appropriate size at a density of 5 × 10⁶ cells/ml in serum-free medium. After 30 min of incubation at 37°C, apoptosis was induced by treatment with 3% CD95-L-containing culture supernatant from CD95-L-expressing N2A cells (42). For the experiments represented in Fig. 1, cells were harvested by centrifugation (500 × g for 5 min at 4°C), washed once in ice-cold phosphate-buffered saline (PBS), and resuspended in cell lysis buffer A (clbA: 0.5% NP-40, 1% Triton X-100, 50 mM Tris-HCl, pH 7.5) or clbA50 (clbA supplemented with 50 mM NaCl) supplemented with protease inhibitors (Complete; Roche) and phosphatase inhibitors (10 mM NaF and 1 mM Na-vanadate). After centrifugation (20,000 × g for 10 min at 4°C), the supernatant was frozen in liquid N₂ and the pellet was resuspended in sodium dodecyl sulfate (SDS)-lysis buffer (50 mM Tris-HCl, pH 8.0, 0.5% SDS, 1 mM dithiothreitol) and heated at 95°C for 10 min. The cell debris was removed by centrifugation at 20,000 × g for 10 min. S-20 extracts for *in vitro* phosphorylation assays were prepared at the indicated times after CD95-L treatment, and the assay was performed as described previously (24).

For the detection of extracellular DEK, medium was collected from cultures treated to undergo apoptosis for the time periods indicated. The medium was centrifuged twice for 5 min at 20,000 × g, and the proteins were precipitated by using methanol-chloroform as described below. For immunoprecipitation of the radiolabeled protein, Jurkat cells were harvested by centrifugation (500 × g for 5 min at 4°C) and washed twice with ice-cold PBS and once with hypotonic buffer (20 mM NaCl, 20 mM HEPES, pH 7.6, 5 mM MgCl₂, protease inhibitors, and phosphatase inhibitors NaF and Na-vanadate), followed by incubation in hypotonic buffer (supplemented with 0.5% NP-40 and protease and phosphatase inhibitors) for 15 min on ice at a cell density of 2 × 10⁷ cells/ml. The soluble material (cytosol/nucleosol) was recovered by centrifugation (500 × g for 5 min at 4°C). The insoluble material was either dissolved in 2% SDS and subjected to gel electrophoresis or resuspended in hypotonic buffer containing 450 mM NaCl for the immunoprecipitation of chromatin-bound DEK. In the latter case, the suspension was incubated for 15 min on ice, insoluble material was pelleted (1,000 × g for 10 min), and the supernatant was incubated with DEK-specific antibodies. For the detection of modified DEK in immunoblots, proteins of the cytosolic/nucleosolic fraction were immediately precipitated with methanol-chloroform as described previously (61). The precipitated material was dissolved in 2% SDS for gel electrophoresis. For immunoprecipitation, 5 μg of affinity-purified polyclonal DEK antibodies was used for the equivalent of 1 × 10⁶ cells. After 1 h of incubation on ice, 30 μl of a 50% protein A-Sepharose suspension (Amersham Pharmacia) was added and the mixture was rolled at 4°C for another hour. The immune complexes were washed three times with 1 ml each of extraction buffer (450 mM NaCl, 20 mM HEPES, pH 7.4, 0.5 mM MgCl₂), followed by dissociation from the beads with 2% SDS and 5% β-mercaptoethanol at 37°C for 1 h. The samples were separated by SDS-polyacrylamide gel

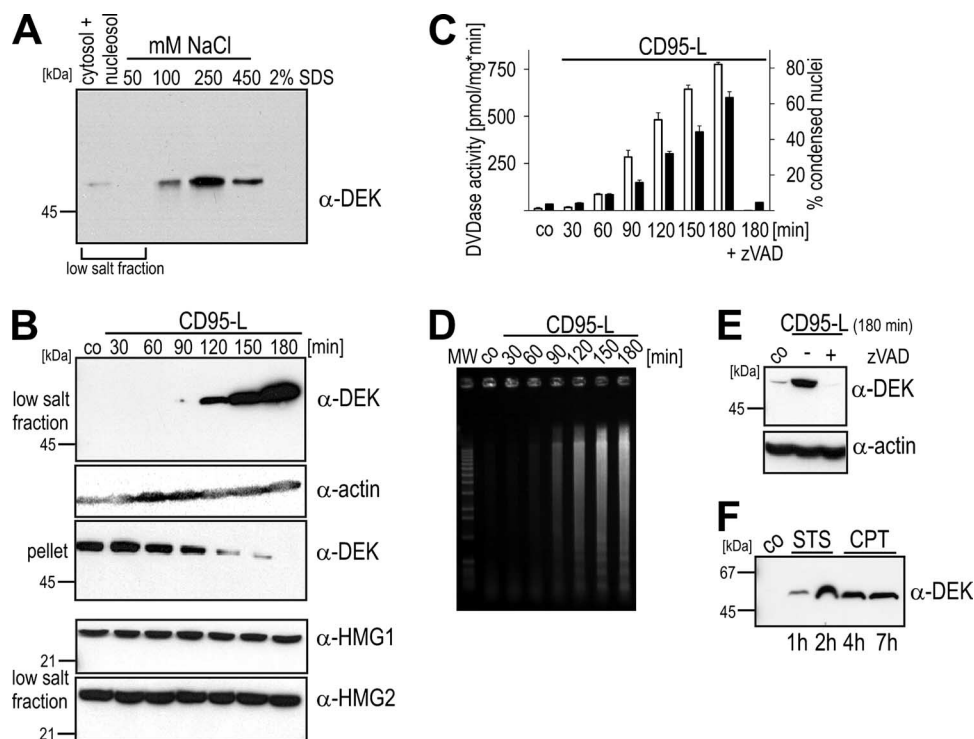


FIG. 1. DEK is released from nuclei of cells undergoing apoptosis. (A) Fractionation of untreated Jurkat E6-1 cells. The fraction containing cytosol and nucleosol was obtained by incubating cells with clbA containing 1% Triton X-100–0.5% NP-40. The pellet containing the nuclei and chromatin-bound proteins was treated with the indicated concentrations of NaCl. The final pellet was solubilized with 2% SDS. Equal aliquots of all fractions were analyzed by immunoblotting with monoclonal DEK-specific antibodies (α -DEK). The bracket indicates the low-salt fraction used for experiments represented in panels B, D, E, and F. (B) Immunoblot analysis of extracts from Jurkat cells undergoing apoptosis. Cells were treated with CD95-L (3%) for the indicated times and lysed in clbA buffer supplemented with 50 mM NaCl (low-salt fraction). The remaining pellet was dissolved in sample buffer containing 0.5% SDS (pellet). Immunoblot analysis was performed with monoclonal antibodies specific for DEK (α -DEK), HMG1 (α -HMG1), and HMG2 (α -HMG2) as indicated. Antiactin (α -actin)-specific antibodies served as a loading control. (C) Time course of nuclear condensation and caspase-3-like/caspase-7-like activity in CD95-L-treated Jurkat cell cultures. Nuclei were stained with Hoechst 33342, and cells with condensed nuclei were scored as apoptotic (open bars). Caspase-3-like/caspase-7-like activity was measured fluorometrically by DEVD-afc cleavage (filled bars). Measurements were carried out in triplicate. Error bars indicate standard deviations. (D) Time course of DNA laddering in Jurkat cell cultures treated with CD95-L. Low-salt extracts were prepared as described above for panel B, and oligonucleosomal fragments were isolated by ethanol precipitation and visualized by agarose gel electrophoresis. (E) Release of DEK is caspase dependent. Cells were treated with CD95-L for the indicated time in the presence (+) or absence (–) of the pan-caspase inhibitor zVAD-fmk (20 μ M). Extracts were obtained as described above for panel B. Samples were analyzed by immunoblotting with monoclonal DEK-specific antibodies. (F) Immunoblot analysis of extracts from untreated (co, control) cells or from cells treated with staurosporine (STS; 0.5 μ M) and camptothecin (CPT; 5 μ M) for the indicated times. Cells were lysed in clbA50 as described above for panel A and analyzed with monoclonal DEK-specific antibodies.

electrophoresis (PAGE), blotted to nitrocellulose (Schleicher & Schuell), and analyzed by autoradiography and immunoblotting.

Immunofluorescence microscopy. For the detection of phosphorylated γ H2AX foci, HeLa cells treated with neocarzinostatin were fixed in PBS containing 4% paraformaldehyde for 10 min at room temperature, followed by two washes in PBS and one in PBS-50 mM NH_4Cl for 10 min each. Cells were permeabilized with 0.2% Triton in PBS for 5 min at room temperature. After extensive washings with PBS, coverslips were incubated with 1% bovine serum albumin (BSA) in PBS for 30 min and then with anti-phospho H2AX antibody diluted 1:500 in PBS containing 10% normal goat serum for 1 h at room temperature. Alexa Fluor 568-conjugated goat anti-mouse immunoglobulins were used as secondary antibodies at a dilution of 1:400. γ H2AX-positive foci were visualized by laser scanning confocal microscopy by using a Zeiss LSM510 Meta microscope. Identical settings were used for each experiment. z stacks consisting of 10 sections (0.6- μ m interval) were recorded. Image analysis was performed on maximum intensity projections of the six z planes by using ImageJ. The mean signal intensity of the nuclei was determined for at least 200 nuclei per experimental condition.

Apoptosis assays. (i) Chromatin condensation. HeLa cells were seeded at a density of 1×10^5 /ml 24 h prior to the experiment. Jurkat cells were plated at a density of 2.5×10^5 /ml 30 min prior to the experiment in 96-well plates, followed

by treatment with camptothecin (Sigma), etoposide (Sigma), neocarzinostatin (Sigma), CD95-L (42), or lz-TRAIL (57) at the concentrations indicated. After 12 h, cells were fixed with 5% formaldehyde, stained with 1.5 μ g/ml Hoechst 33342 and inspected microscopically. Cells with characteristically condensed or fragmented nuclei were scored as apoptotic.

(ii) Caspase activity assay. A total of 3×10^5 HeLa cells were seeded in six-well plates 24 h prior to the experiment and treated with camptothecin (500 nM), etoposide (50 μ M), or neocarzinostatin (300 ng/ml). At the indicated time points, the cells were placed on ice and after the addition of a $3\times$ protease inhibitor solution in PBS (amounting to one-third of the culture volume), cells were gently scraped off the dish and collected by centrifugation. Cells were lysed in 25 mM HEPES, pH 7.5, 5 mM MgCl_2 , 1 mM EGTA, and 0.5% Triton X-100, and the cleavage of DEVD-7-amino-4-trifluoromethyl coumarin (afc) (40 μ M) was monitored fluorometrically in reaction buffer (50 mM HEPES, pH 7.5, 10 mM dithiothreitol, 1% sucrose, 0.1% CHAPS {3-[(3-cholamidopropyl)-dimethylammonio]-1-propanesulfonate}) over a period of 20 min at 37°C, with a λ_{ex} (excitation wavelength) value of 390 nm and a λ_{em} (emission wavelength) value of 505 nm. The activity was calibrated by using afc standard solutions. Measurements were run in triplicate.

Caspase-3 processing was detected in whole-cell lysates by immunoblot anal-

ysis using neo-epitope-specific antibodies recognizing the large fragment (p17/p19) of activated caspase-3.

(iii) DNA laddering. Low-salt extract corresponding to 8×10^5 Jurkat cells was deproteinated by treatment with 100 $\mu\text{g/ml}$ proteinase K for 2.5 h at 37°C. The DNA was precipitated with 2.5 volumes of ethanol at -20°C overnight and recovered by centrifugation ($20,000 \times g$ for 20 min at 4°C). After RNase treatment (100 $\mu\text{g/ml}$, 37°C, 30 min), oligonucleosomal fragments were visualized by agarose gel electrophoresis.

Sucrose density gradient centrifugation. Sucrose density gradient analyses were essentially performed as described previously by Kappes et al. (24). Briefly, Jurkat cells were washed twice in equilibrated serum-free RPMI medium and seeded at a density of 5×10^6 cells/ml. After 2.5 h of apoptosis induction by 3% CD95-L, cells were harvested by centrifugation, washed with ice-cold PBS, and lysed with cbaA50 buffer. Soluble material (low-salt fraction) was separated by centrifugation ($1,000 \times g$ for 10 min at 4°C) and layered on sucrose density gradients (5% to 40% sucrose prepared in cbaA50 without NP-40 and Triton X-100). After 14 h of centrifugation at $160,000 \times g$ (SW-41 rotor; Beckman), gradients were fractionated and individual samples were analyzed by agarose electrophoresis and immunoblotting.

Poly(ADP-ribosyl)ation and PAR-binding assays. (i) **in vitro poly(ADP-ribosyl)ation of recombinant DEK.** Reactions were carried out in a volume of 50 μl containing 100 mM Tris-HCl, pH 7.8, 10 mM MgCl_2 , 1 mM dithiothreitol, and 10 μM of the double-stranded octameric palindromic oligonucleotide GGAA TTCC (Invitrogen) in the presence of DEK and NAD^+ (Sigma) at 1 mM (Fig. 3A) or the various concentrations indicated (see Fig. S3 in the supplemental material). As a positive control, 50 pmol recombinant p53 was included (34). The reactions were started by adding 565 ng of recombinant human PARP1 (100 nM) and incubated at 37°C for 15 min on a shaker. Recombinant human PARP1, human p53, and DEK were overexpressed in insect cells by using the baculovirus system as described previously (15, 24). The reactions were stopped by the addition of an equal volume of $2 \times$ PAGE loading buffer, followed by 5 min of incubation at 95°C. For the electrophoretic mobility shift assay (EMSA) and the topology and aggregation assays, samples were further processed as described below. The proteins were blotted onto nitrocellulose by using a wet blot chamber (Bio-Rad), and the filters were then incubated in Tris-buffered saline-Tween (TBS-T) with 5% (wt/vol) skim milk powder at room temperature. Incubations with primary antibodies were in TBS-T with milk at 4°C overnight. Filter washings and incubations with peroxidase-coupled secondary antibodies were in TBS-T only. PAR was detected with monoclonal antibody 10H at a 1:200 dilution. For the detection of DEK and PARP1, filters were stripped and reprobed with polyclonal DEK-specific antibodies (1:10,000) and monoclonal PARP-specific antibodies CII10 (1:5), respectively.

(ii) **PAR overlay blot.** Increasing amounts of recombinant DEK (0 to 50 pmol) and BSA (100 pmol) were separated by 14% PAGE and blotted onto nitrocellulose by semidry transfer (Amersham Biosciences). Filters were washed in TBS-T and incubated overnight at 4°C in TBS-T containing 5 nmol (1 μM) of purified PAR. Filters were subsequently washed in TBS-T-1 M NaCl and TBS-T-5% (wt/vol) skim milk powder. The detection of bound PAR polymers was performed as described above by using 10H antibody, followed by Ponceau S staining to visualize the proteins.

Assessment of DNA repair by FADU. The fluorometric analysis of DNA unwinding (FADU) assay is based on the time-dependent denaturation of DNA under moderate alkaline conditions. Denaturation starts from DNA breakpoints (single- and double-strand breaks) and is terminated by neutralization. DNA that remains double stranded is detected by the addition of the intercalating dye SYBR green, a fluorescent compound specific for double-stranded DNA, and measured fluorometrically. Here, we employed an automated version of the FADU assay that ensures very reliable and reproducible results (A. Moreno-Villanueva et al., submitted for publication). Briefly, HeLa cells ($2.5 \times 10^5/\text{ml}$) were subjected to a short pulse treatment with camptothecin (250 nM), etoposide (30 μM), or neocarzinostatin (2 $\mu\text{g/ml}$) at 37°C for 5 min. Cells were then collected by centrifugation, resuspended in medium containing 5% FCS, and divided into equal 100- μl aliquots corresponding to 6×10^4 cells. Aliquots were then incubated at 37°C for different times to allow DNA repair. Cells were then collected on ice and subjected to the FADU procedure by using a pipetting robot (Genesis RSP 100; Tecan). The fluorescence intensity values are a measure of the amount of double-stranded DNA present in each sample. DNA repair is calculated as the percent reduction of the treatment-induced loss of double-stranded DNA. Values above 100% indicate that cells also repair the basal DNA lesions present in the absence of treatment.

EMSA and topology and aggregation assays. EMSAs and topology assays were carried out essentially as described previously by Kappes et al. (24, 25). Aggregation assays were performed according to the method of Böhm et al. (5). For in

vitro poly(ADP-ribosyl)ation, recombinant His-DEK was first dephosphorylated with λ -phosphatase according to the manufacturer's instructions (NEB) and treated as described above. Poly(ADP-ribosyl)ated DEK was swim filter dialyzed in the presence of purified BSA against nE300 (20 mM HEPES, pH 7.6, 300 mM NaCl, 10 mM sodium bisulfite, and 1 mM EDTA) for 90 min at 4°C prior to being used in the assays.

RESULTS

DEK is released from chromatin during apoptosis. We set out to determine whether the induction of apoptosis affects the characteristic behavior of DEK as a chromatin-binding protein. In control Jurkat cells, DEK elutes from chromatin at 250 mM NaCl. No DEK is present in the cytosolic/nucleosolic fraction and a fraction isolated at low ionic strength (50 mM NaCl) (Fig. 1A), confirming previous data obtained with HeLa cells (23). In contrast, increasing amounts of DEK were recovered in a low-salt extract of Jurkat cells undergoing apoptosis triggered by CD95-L (29). This effect seems to be unique to DEK since no change in the recovery of HMG1 and HMG2 is observed under the same conditions (Fig. 1B). DEK's appearance in low-salt extracts coincides with the progression of several apoptosis parameters, such as chromatin condensation, caspase-3/caspase-7 activity, and oligonucleosomal DNA laddering (Fig. 1C and D), and is dependent on caspase activity, as shown by experiments performed in the presence of the caspase inhibitor zVAD-fmk (Fig. 1E). The increased recovery of DEK under low-salt conditions is also observed in cells undergoing apoptosis after staurosporine or camptothecin treatment (Fig. 1F).

DEK released from chromatin in apoptosis is posttranslationally modified. According to our previous in vitro studies, DEK's interaction with chromatin is modulated by phosphorylation (24, 53). We therefore wished to assess whether phosphorylation contributes to the release of DEK from apoptotic nuclei. To this end, we examined the phosphorylation level of DEK in subcellular fractions of cells treated with CD95-L. DEK present in the soluble fraction (cytosol plus nucleosol) was highly phosphorylated during apoptosis, as revealed by the immunoprecipitation of the radiolabeled protein (Fig. 2A, bottom left panel). Further extraction of the nuclear pellet with 450 mM NaCl yielded chromatin-bound DEK, evincing a significantly reduced level of phosphorylation compared to the level for control cells (compare chromatin fractions with and without CD95-L in Fig. 2A). These results are consistent with our proteome analysis that was performed on nuclear pellets of a cell-free apoptosis reaction and showed the hypophosphorylation of DEK (53). These data further indicate that during apoptosis, the cellular pool of DEK separates into two fractions, a soluble hyperphosphorylated one that is released from chromatin and a second hypophosphorylated one that is retained on apoptotic chromatin. Additional in vitro studies suggest that apoptotic phosphorylation of DEK is carried out by kinases distinct from the previously described CK2. These kinases are not susceptible to inhibition by 4,5,6,7-tetrabromobenzotriazole (39) and await further characterization (see Fig. S1 in the supplemental material).

Interestingly, less DEK was detected in the extracts used for immunoprecipitation than in the low-salt fraction shown in Fig. 1B and, furthermore, these extracts contained phosphorylated DEK species of higher molecular weights, resulting in a smear

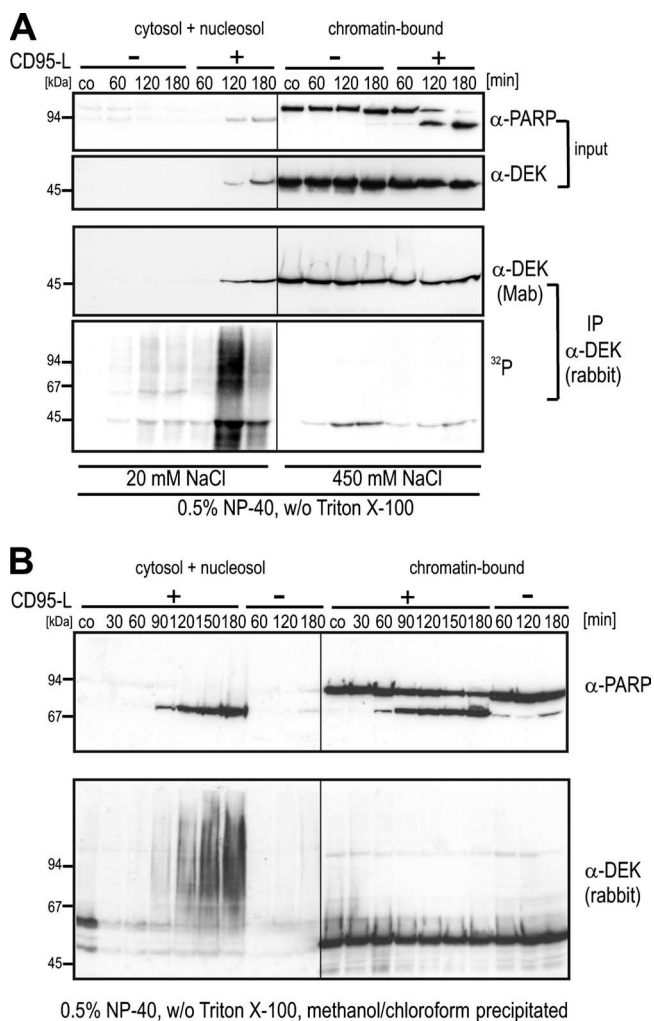


FIG. 2. Phosphorylation and high-molecular-weight modification of DEK in apoptotic cells. (A) Jurkat cells were pulse labeled with [³²P]orthophosphate and either left untreated or incubated in the presence of 3% CD95-L. At the indicated time points, apoptotic and control (co) cells were harvested and lysed with hypotonic buffer containing 0.5% NP-40 to yield soluble proteins (cytosol/nucleosol). The remaining nuclear and chromatin structures were extracted with 450 mM NaCl (chromatin bound). Equal amounts of the individual fractions were analyzed by immunoblotting with PARP1- or DEK-specific antibodies (α-PARP or α-DEK). Immunoprecipitations (IP) were carried out by the addition of 5 μg affinity-purified DEK-specific polyclonal antibodies to the individual fractions in the presence of 0.5% NP-40. Immune complexes were analyzed by autoradiography (lower panel) and by immunoblotting with DEK-specific monoclonal antibodies (Mab) (upper panel). (B) Jurkat cells, either untreated (–) or stimulated to undergo apoptosis with 3% CD95-L (+) for the indicated times, were lysed with hypotonic buffer containing 0.5% NP-40 to yield soluble proteins (cytosol and nucleosol). The remaining nuclear structures were extracted with 450 mM NaCl (chromatin bound). Individual fractions were precipitated immediately with methanol-chloroform and subjected to immunoblot analysis with DEK-specific polyclonal antibodies (lower panel). The same blot was reprobbed with PARP1-specific monoclonal antibodies to monitor PARP1 cleavage as a marker for apoptosis progression (upper panel).

in the autoradiogram (Fig. 2A, left panel). A systematic comparison of different lysis and sample preparation procedures indicated that the recovery of apoptotically released DEK strongly depends on buffer composition and sample handling. High-molecular-weight DEK species appeared exclusively in

cytosolic/nucleosolic fractions (Fig. 2B, bottom left panel) prepared in 0.5% NP-40 and precipitated immediately with methanol-chloroform (61), but did not appear if Triton X-100 was present and/or samples were incubated on ice (see Fig. S2 in the supplemental material).

The unstable nature of these DEK species, their molecular weight range, and the lack of discrete bands in immunoblots were suggestive of poly(ADP-ribosylation). Supporting this assumption, DEK is poly(ADP-ribosylated) in *in vitro* assays using recombinant purified PARP1 and NAD⁺, the direct substrate of this modification reaction (Fig. 3A, top and middle panels). The poly(ADP-ribosylation) of DEK occurred at physiological NAD⁺ concentrations and was augmented with increasing substrate concentrations, underscoring the specificity of the reaction (see Fig. S3 in the supplemental material). Accordingly, immunoprecipitation experiments using DEK- or PAR-specific antibodies showed that DEK is found poly(ADP-ribosylated) *in vivo* in apoptotic cells (Fig. 3B). The level of modification detected by this method was low compared to the immediate precipitation of modified DEK species from cell lysates, most likely due to the degradation of the typically unstable PAR moieties during antibody incubation. The association between DEK and PARP1 is further supported by sucrose gradient density studies of micrococcal nuclease-digested chromatin. Here, DEK and PARP1 colocalize preferentially to regions of active chromatin present in the soluble supernatant of the micrococcal nuclease reaction (see Fig. S4 in the supplemental material). As a consequence of poly(ADP-ribosylation), DEK loses both its DNA-binding activity and the ability to alter DNA topology as shown by EMSA, aggregation assays, and topology assays (Fig. 3C).

Further, the ability of DEK to interact noncovalently with PAR polymers was demonstrated by a PAR overlay assay, in which recombinant His-tagged DEK blotted onto nitrocellulose was incubated with purified PAR (Fig. 3D, top panel). High amounts of BSA (100 pmol versus 50 pmol of DEK) showed no PAR binding (for a presentation of a further control for the specificity of DEK's binding to PAR, see Fig. S5 in the supplemental material).

DEK is involved in repair of DNA lesions induced by radiomimetic drugs and topoisomerase poisons. Since the activation of PARP1 and the synthesis of ADP-ribose polymers are early events in DNA damage signaling and repair pathways (8), we were interested in determining whether DEK is involved in these functions. We therefore created stable Jurkat and HeLa cell lines with impaired DEK expression utilizing lentiviral shRNA delivery systems. DEK expression was significantly decreased in these cells, more effectively so in HeLa cells than in Jurkat cells (see Fig. S6 in the supplemental material). Furthermore, we observed different knockdown levels by using the commercially available monoclonal DEK-specific antibody versus a rabbit polyclonal DEK-specific antibody (data not shown). These antibodies also differed in their abilities to detect modified DEK (see Fig. S7A, S7B, and S7C in the supplemental material).

The DNA repair activity of DEK knockdown cells was compared to that of control cells by two independent approaches. First, we analyzed the induction and persistence of histone H2AX phosphorylation on serine 139, a well-established marker of DNA double-strand breaks (54). Cells were sub-

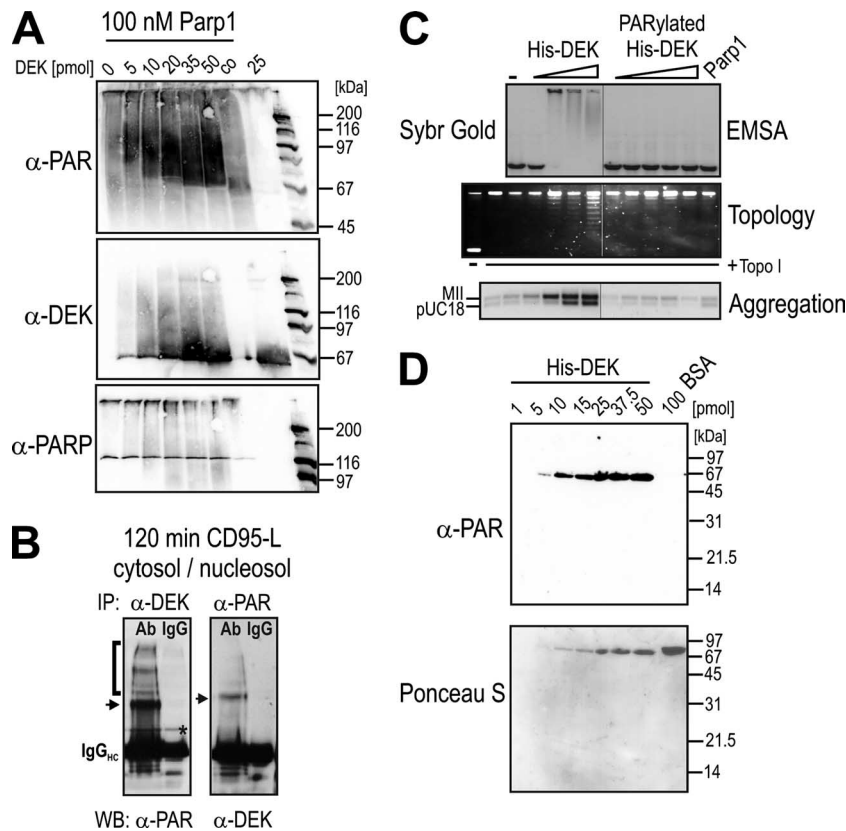


FIG. 3. Poly(ADP-ribosylation) of DEK in vitro and in apoptotic cells. (A) In vitro poly(ADP-ribosylation) of DEK. Five pmol (100 nM) PARP1 was incubated with increasing amounts of DEK (0, 5, 10, 20, 35 and 50 pmol) in the presence of 1 mM NAD^+ . Fifty pmol recombinant p53 was used as a positive control (co). The samples were subjected to 8% SDS-PAGE and transferred onto a nitrocellulose membrane. Poly(ADP-ribosylated) proteins were detected using monoclonal PAR-specific antibodies 10H (α -PAR) (upper panel). In addition, DEK was detected by using polyclonal DEK-specific antibodies (α -DEK) (middle panel) and PARP1 or the automodification of PARP1 was monitored by CII-10 antibody (lower panel). (B) DEK released by apoptotic cells is poly(ADP-ribosylated) in vivo. Jurkat cells were induced to undergo apoptosis by the addition of 3% CD95-L for 2 h. Cells were harvested and lysed in hypotonic buffer containing 0.5% NP-40 to extract soluble cytosolic and nucleosolic structures and proteins. For DEK- or PAR-specific immunoprecipitations (IP), 3×10^6 cells were treated with 10 μg of affinity-purified DEK- or PAR-specific polyclonal antibodies (Ab) or 10 μg of nonspecific rabbit immunoglobulin G (IgG) for 30 min at 4°C. After the addition of a protein A-agarose slurry for 30 min, immune complexes were washed with hypotonic buffer and analyzed by SDS-PAGE and immunoblotting with DEK- and PAR-specific polyclonal antibodies, respectively. The position of the IgG heavy chain (IgG_{HC}) is indicated. Arrows indicate the positions of poly(ADP-ribosylated) DEK or PAR attached to DEK. The bracket indicates high-molecular-weight poly(ADP-ribosylated) DEK species. The asterisk marks a band of unknown nature. WB, Western blot. (C, upper panel) EMSA. A total of 0.04 pmol linearized SV40 DNA was incubated with increasing amounts (1, 2, 4, and 8 pmol) of poly(ADP-ribosylated) or untreated DEK. As a control, PARP1 in concentrations present in the in vitro poly(ADP-ribosylation) reaction was used. Nucleoprotein complexes were analyzed by agarose gel electrophoresis and visualized by SYBR gold staining. (Middle panel) Topology assay. Increasing amounts of untreated and poly(ADP-ribosylated) DEK (0.5, 1, 2, 4, and 8 pmol) were incubated with 15 ng of SV40 DNA in the presence of topoisomerase 1 (1 U). Samples were deproteinized and analyzed by agarose gel electrophoresis. (Lower panel) Aggregation assay. Increasing amounts of untreated or poly(ADP-ribosylated) DEK (0.5, 1, 2, 4 and 8 pmol) were incubated with 3 ng of radiolabeled DNA (MII, AT-rich SAR/MAR fragment of human topoisomerase 1 [Topo 1] gene; pUC18, control DNA). Samples were centrifuged, and pellets were analyzed by agarose gel electrophoresis and exposed to autoradiography. PARP1 served as a control as above. (D) DEK binds PAR noncovalently. Increasing amounts of DEK (1, 5, 10, 15, 25, 37.5, and 50 pmol) were separated by 14% SDS-PAGE and transferred onto a nitrocellulose membrane. A total of 100 pmol of BSA served as a negative control. The membrane was subsequently incubated with 5 nmol (1 μM) of unfractionated PAR, and nonspecific binding was disrupted by high-salt washes containing 1 M NaCl. Bound polymers were detected by using PAR-specific antibodies 10H (upper panel). Ponceau staining was used to visualize blotted proteins (lower panel).

jected to a pulse treatment with neocarzinostatin (36) and fixed immediately or allowed to recover for 4 h or 8 h prior labeling with γH2AX -specific antibodies (Fig. 4A). γH2AX -specific signals in the nucleus were quantified by confocal microscopy. DNA repair was expressed as the decrease of the averaged nuclear signal at 4 h and 8 h as a percentage of the signal intensity obtained immediately after treatment. In cells with downregulated DEK expression, the loss of γH2AX -specific staining was markedly reduced, indicating that positive foci

persisted over time (Fig. 4B and C). Similar observations were also made for cells treated with an alkylating DNA-damaging agent, *N*-methyl-*N'*-nitro-*N*-nitrosoguanidine (data not shown). It is also noteworthy that no significant increase in γH2AX -specific staining was observed after DEK knockdown in the absence of genotoxic stress.

As a second approach, we used an automated version of the FADU assay, a fast and highly reproducible fluorometric method for quantifying both single- and double-strand DNA

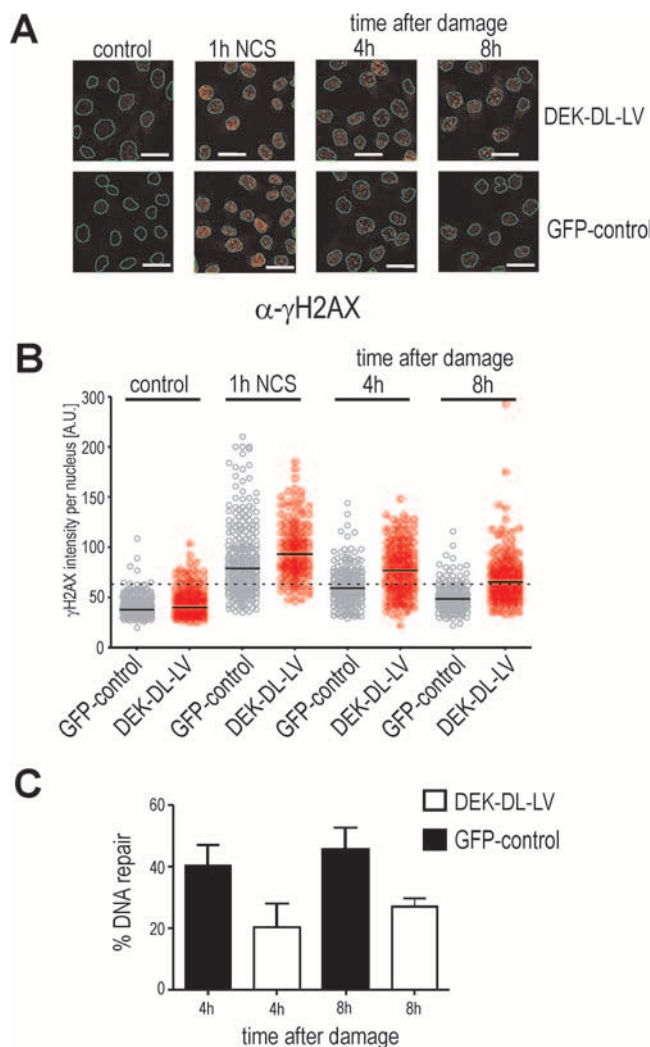


FIG. 4. Downregulation of DEK leads to persisting γ H2AX-positive foci. (A) Immunofluorescence analysis of γ H2AX-positive foci in DEK-DL-LV and GFP-control cells. Cells were treated with 30 ng/ml neocarzinostatin (NCS) for 1 h, either fixed immediately or transferred to fresh medium, and incubated for 4 h or 8 h at 37°C prior to fixation. Cells were immunolabeled with antibodies specific for the phosphorylated form of H2AX (α - γ H2AX). The figure shows representative confocal images. Bar, 20 μ m. (B) Distribution of γ H2AX-specific signal intensity per nucleus in DEK-DL-LV and GFP-control cells treated as indicated. Image analysis was performed on maximum intensity projections of six confocal z planes. At least 200 nuclei were evaluated per experimental condition. The scatter plot shows one representative data set. The dotted line indicates the intensity threshold for damaged nuclei. A.U., arbitrary units. (C) DNA repair activity in DEK-DL-LV and GFP-control cells. The number of nuclei with signal intensities above the threshold level set for in panel B were counted at the indicated times and expressed as a percentage of damaged nuclei present after 1 h of treatment with neocarzinostatin. Bars represent the average of three independent experiments. Error bars indicate standard deviations.

breaks (Moreno-Villanueva et al., submitted). Repair activity was compared in control and DEK knockdown cells challenged either with neocarzinostatin or with the topoisomerase inhibitors camptothecin and etoposide (Fig. 5). Corroborating the data obtained by γ H2AX immunostaining, DEK knockdown

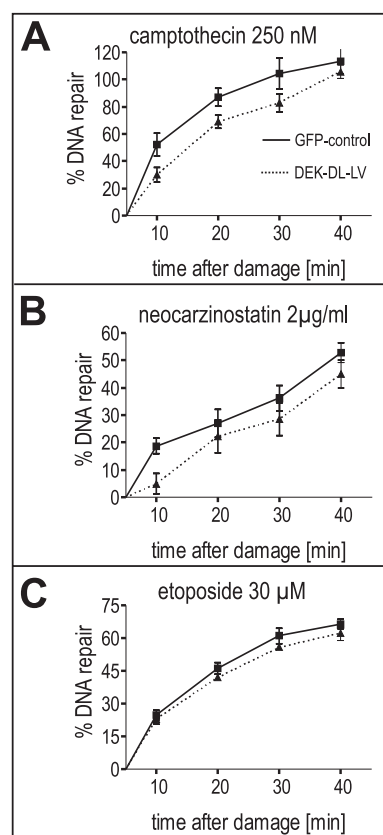


FIG. 5. Interference with DEK expression inhibits the repair of DNA strand breaks. HeLa cells with a stable, lentivirus-mediated knockdown of DEK expression, DEK-DL-LV, and the corresponding GFP-expressing control cell line were treated with camptothecin (A), etoposide (C), or neocarzinostatin (B) for 5 min at 37°C at the indicated concentrations. Cells were washed, incubated in fresh medium and allowed to repair damaged DNA at 37°C. At the indicated time points, cells were lysed and the amount of remaining intact DNA was determined by using an automated version of the FADU assay. DNA repair was calculated as a percent reduction of the treatment-induced loss of double-stranded DNA over time. Data represents the average of a minimum of three independent experiments. Error bars indicate standard deviations.

cells displayed a reduced ability to resolve DNA strand breaks compared to the controls. Interestingly, the magnitude of the effect was small relative to the difference in persistence of γ H2AX-positive foci, suggesting that DEK may be more involved in the repair of double-strand breaks by nonhomologous end joining and homologous recombination rather than in base excision repair, which is the end point detected by the FADU assay.

Inhibition of DEK expression sensitizes cells toward genotoxic stress. Having established that loss of DEK interferes with the signaling involved in DNA repair or DNA repair itself, we investigated whether this loss would also lower the threshold for DNA damage-induced cytotoxicity. Apoptosis induced by camptothecin, etoposide, and neocarzinostatin was assessed in DEK knockdown and control HeLa cells by scoring for condensed nuclei. As shown in Fig. 6, interference with DEK expression results in a marked sensitization toward these DNA-damaging agents, while it had no influence on the re-

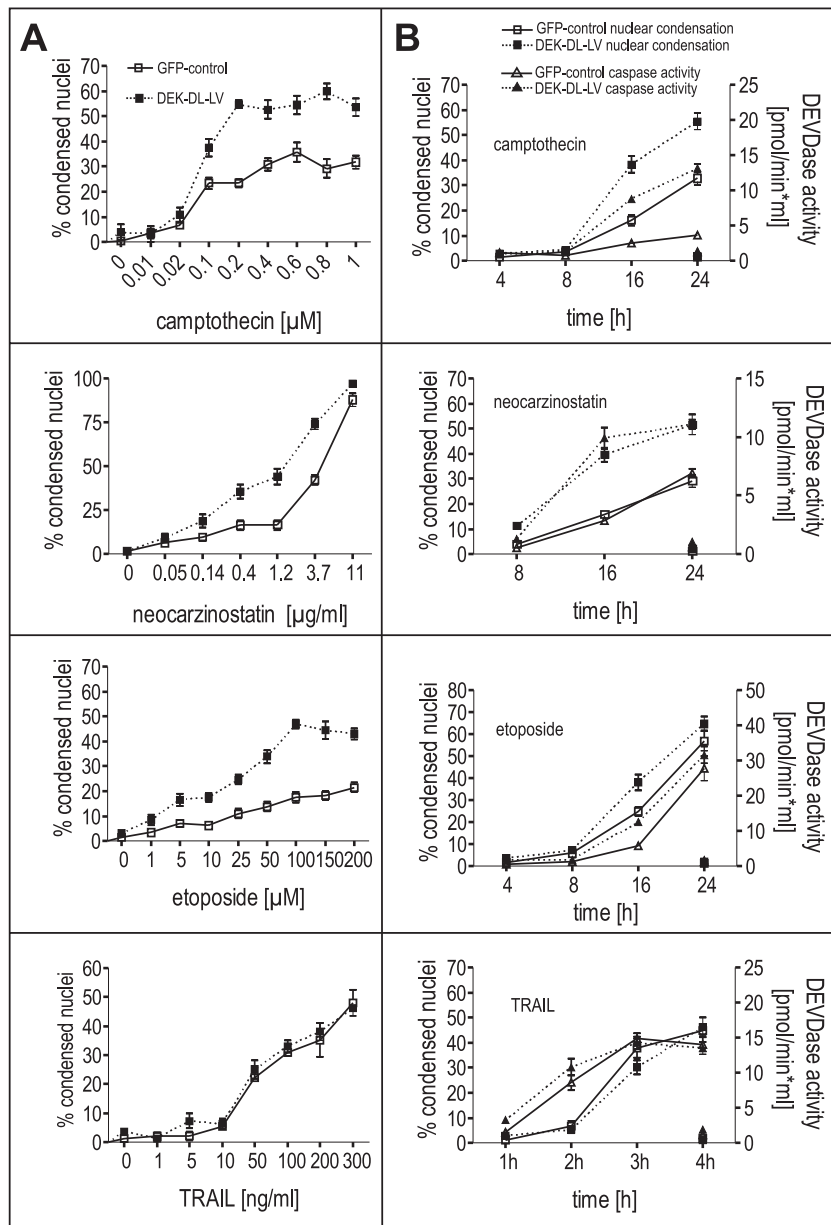


FIG. 6. DEK knockdown sensitizes cells to DNA damage-induced apoptosis. (A) DEK-DL-LV cells and GFP-control cells were treated with camptothecin or neocarzinostatin for 24 h, etoposide for 16 h, or TRAIL for 4 h at the indicated concentrations. Cells were fixed, stained with Hoechst 33342, and inspected by fluorescence microscopy. Cells with condensed or fragmented nuclei were scored as apoptotic. Measurements were performed in triplicate. (B) Time course of apoptosis and caspase-3/caspase-7-like activation in DEK-DL-LV and GFP-control cells. Cells were treated with either 500 nM camptothecin, 50 μM etoposide, 300 ng/ml neocarzinostatin, or 300 ng/ml TRAIL for the indicated times. Aliquots were taken for microscopic evaluation of apoptosis as described above for panel A, and caspase-3/caspase-7-like activity was measured for the corresponding lysates by DEVD-afc cleavage (also see Fig. S8 in the supplemental material). Samples from control untreated cells were taken at the end of each time course and showed neither nuclear condensation nor caspase activation. Measurements were performed in triplicate. Error bars indicate standard deviations.

sponse of the cells to death receptor-induced apoptosis triggered by TRAIL. Time-dependent measurement of caspase-3-like/caspase-7-like activity revealed an increased activation of caspases in DEK-silenced cells (Fig. 6, right panels; see Fig. S8 in the supplemental material). Similar results were obtained in Jurkat DEK-knockdown cells in which different sequences of the DEK gene were targeted by the lentiviral shRNA con-

structs, confirming the specificity of these effects (see Fig. S9 in the supplemental material).

DEK modified and released during apoptosis is potentially immunogenic. In addition to its possible involvement in DNA repair and DNA damage signaling, DEK was shown to be a potent autoantigen and was also proposed to be a mediator of inflammation (35). Therefore, the presence of posttranslational-

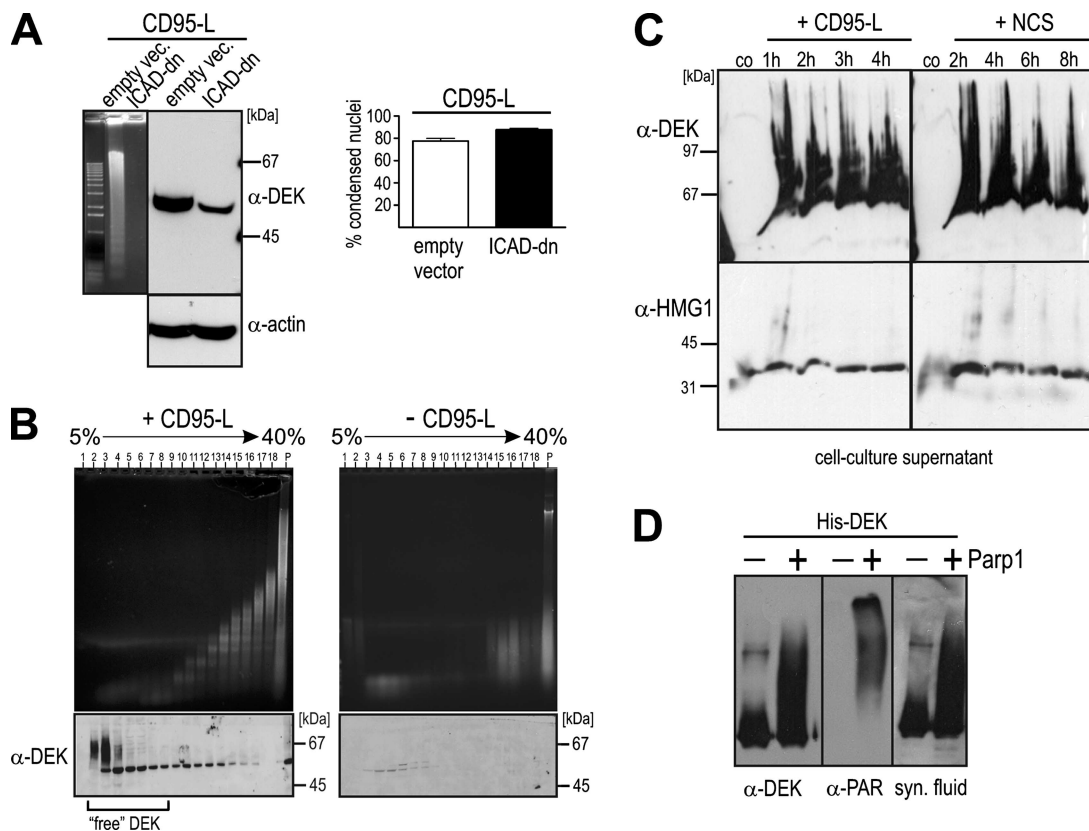


FIG. 7. Poly(ADP-ribosyl)ated DEK is released by apoptotic cells and is recognized by autoantibodies from synovial fluids. (A) Apoptotic ICAD-dn-expressing cells release DEK in the absence of DNA laddering. Extracts from Jurkat ICAD-dn-expressing cells and the parental cell line treated with CD95-L (3% for 2.5 h) were obtained by lysis in clbA50 and analyzed for the presence of oligonucleosomal DNA fragments by agarose gel electrophoresis (left panel) and DEK by immunoblotting using monoclonal DEK-specific antibodies (α -DEK and α -actin). ICAD-dn-expressing cells undergo CD95-dependent apoptosis (right panel). Cultures of Jurkat cells stably expressing ICAD-dn and the control cell line (empty vector) were treated with CD95-L (3%) for 2.5 h. Cultures were stained with Hoechst 33342, and cells with condensed nuclei were scored as apoptotic. Measurements were performed in triplicate. Error bars indicate standard deviations. (B) Released DEK occurs in a DNA-free, modified form in sucrose density gradients of apoptotic chromatin fragments. Jurkat E6-1 cells were incubated with (+) 3% CD95-L for 2.5 h, and soluble material was harvested by extracting cells with either clbA or hypotonic buffer (as for Fig. 1 or 2B). Soluble chromatin fragments and proteins were layered on sucrose density gradients (5% to 40% sucrose in the appropriate buffer without NP-40 and Triton X-100) and centrifuged for 14 h ($160,000 \times g$ at 4°C) (SW-41 rotor; Beckman). Individual fractions were analyzed by agarose gel electrophoresis (1%) for DNA (upper panels) and by immunoblotting as for panel A (lower panels). Positions of the individual fractions are indicated from the top (left) to the bottom (right) of the gradient. The bracket indicates the position of DEK not associated with nucleosomes. Extracts of nonapoptotic Jurkat cells ($-$ CD95-L) served as a control and were obtained and analyzed in the same way. (C) DEK is present in cell culture supernatants of apoptotic cells. Jurkat E6-1 cells were treated to undergo apoptosis with 3% CD95-L or $1 \mu\text{g/ml}$ neocarzinostatin (NCS). At the indicated time points, aliquots of the culture medium were cleared by centrifugation and precipitated immediately with methanol-chloroform. The samples were analyzed by immunoblotting using DEK-specific polyclonal antibodies (α -DEK). The same samples were analyzed by immunoblotting using HMG1-specific antibodies (lower panel) (α -HMG1). co, control. (D) Poly(ADP-ribosyl)ated DEK is detected by DEK-specific autoantibodies from synovial fluids from JRA/JIA patients. Recombinant His-DEK was poly(ADP-ribosyl)ated in vitro (+ lanes) or left untreated ($-$ lanes). Immunoblots were analyzed by either polyclonal DEK-specific antibodies (α -DEK) or PAR-specific antibodies (α -PAR) or by DEK-specific autoantibodies purified by affinity chromatography from the synovial fluid of a patient affected by JRA/JIA with positive antinuclear antibody status (syn. fluid).

ally modified DEK in soluble, non-chromatin-bound fractions of apoptotic cells could represent a specific portion of the cellular DEK pool that may be extruded into the extracellular milieu during apoptosis and potentially contribute to the proinflammatory and immunogenic functions of this protein.

We therefore wished to detail the apoptotic release of DEK and asked whether DEK is extruded from apoptotic nuclei in association with oligonucleosomal fragments. To this end, we generated Jurkat cells devoid of oligonucleosomal DNA cleavage due to the expression of a dominant-negative inhibitor of the caspase-activated DNase CAD. These cells underwent apoptosis to the same extent as did controls (Fig. 7A; see Fig.

S10 in the supplemental material); however, oligonucleosomal laddering in response to CD95-L was completely suppressed (Fig. 7A, left panel) (44). Immunoblot analysis showed that despite the inhibition of CAD, a significant amount of DEK could still be detected in low-salt extracts (Fig. 7A, right panel). Thus, DEK can be released from nuclei independently of oligonucleosomes, a finding further confirmed by sedimentation analysis in sucrose density gradients (Fig. 7B). While a part of DEK present in low-salt apoptotic extracts comigrated with oligonucleosomes, a substantial amount was found in the top, DNA-devoid fractions of the gradient. DEK present in these fractions is heavily posttranslationally modified, as indi-

cated by the high-molecular-weight smear in the immunoblot. We estimated that about 30% of the total DEK released was found in a free, non-chromatin-bound form.

We next assessed whether the generation of highly modified, soluble DEK could lead to the release of the protein in the cell culture supernatant. Indeed, we could detect extracellular modified DEK regardless of the apoptosis trigger (Fig. 7C). This contributes to the possibility of poly(ADP-ribosyl)ated DEK being exposed to the immune system and acting as a self-antigen. We therefore were interested in whether DEK-specific autoantibodies present in the synovial fluids of JRA/JIA patients (data not shown) were capable of detecting poly(ADP-ribosyl)ated DEK. We indeed found that DEK-specific autoantibodies from synovial fluids efficiently detected poly(ADP-ribosyl)ated DEK (Fig. 7D). In summary, these data support the notion that under conditions of insufficient phagocytic clearance, apoptosing cells may represent a source of highly immunogenic DEK forms and could contribute to the generation of DEK autoantibodies.

DISCUSSION

A number of *in vitro* studies clearly established DEK as a modifier of chromatin superhelical density due to its biochemical properties (2, 25, 58, 59). Concurrently, DEK was shown to have pleiotropic functions in cells, affecting the replication, splicing, and transcription of different genes (9, 27, 33, 45), thus making it difficult to pinpoint the functional targets of DEK in the nucleus. The relevance of DEK in chromatin homeostasis is underscored by its strong association with oncogenesis, while an additional potential role in inflammation is supported by its potent autoantigenic and chemotactic activity. In order to decipher the mechanisms underlying DEK's activity on the genome and to understand how its deregulation may result in disease, more information is needed about the mechanisms regulating the binding of DEK to chromatin *in vivo*.

Here, we show that under stress conditions (e.g., apoptosis), DEK is removed from chromatin, both in association with oligonucleosomes and in a free form. Released DEK is hyperphosphorylated, while the remaining chromatin-associated DEK fraction is significantly less phosphorylated compared to untreated cells. These results are consistent with the existence of a dynamic equilibrium on chromatin between dephosphorylated and phosphorylated DEK, where the dephosphorylated form anchors the phosphorylated one to chromatin via intermolecular interactions, as supported by recent *in vitro* data (24). The second posttranslational modification of DEK that we demonstrate in cells undergoing apoptosis is poly(ADP-ribosylation). This modification, which is traditionally associated with DNA damage, is observed also in cells treated with CD95-L, although this is not a DNA-damaging agent *per se*. However, a transient early burst of PARP1 activity has already been described after the stimulation of death receptors by CD95-L (48), possibly involving the generation of reactive oxygen species and oxidative DNA lesions (52).

Poly(ADP-ribosylation) in concert with phosphorylation leads to the dissociation of DEK from chromatin and abolishes the chromatin folding activity of DEK (this work; 17). DEK also binds isolated ADP-ribose polymers noncovalently with very high affinity. In fact, we were able to identify several

PAR-binding consensus motifs (40) in the DEK primary sequence (data not shown). This noncovalent interaction may contribute in the recruitment of DEK to poly(ADP-ribosyl)ated protein complexes present on chromatin or chromatin fragments.

Taken together (Fig. 8), these data support the notion that apoptosis elicits a specific and unique posttranslational modification pattern of DEK that weakens the binding of DEK to DNA and, due to increased phosphorylation, favors the formation of protein-protein complexes. The detection of such modified DEK and DEK-DNA complexes in soluble fractions and culture supernatants from apoptosing cells suggests that these cells, if not promptly cleared, could become a source of immunogenic DEK. This suggestion is supported by the observation that circulating DEK-autoantibodies from synovial fluids of a JRA/JIA patient efficiently detected poly(ADP-ribosyl)ated DEK (Fig. 7). We recently showed that DEK can be secreted from activated, nonapoptotic macrophages, which represents one possibility for the generation of DEK autoantibodies (35). Cell death could thus provide a second and new pathway besides cell activation and exosomal secretion. DEK release from apoptotic cells could also exacerbate inflammatory reactions. In fact, we have recently demonstrated that DEK present in the extracellular milieu has chemoattractant properties, stimulating the migration of T cells, NK cells, and neutrophils (35). The finding that DEK may be extruded from dying cells extends the similarity between this protein and HMG1, a member of the "high-mobility-group" family of architectural chromatin proteins. Different from DEK, HMG1 is released from necrotic cells and not from apoptotic cells (46). However, this paradigm has been challenged by recent studies reporting the release of HMG1 during apoptosis [3, 22]), which is consistent with the presence of HMG1 in cell culture supernatants from CD95-L- and neocarzinostatin-treated cells (Fig. 7C). HMG1, like DEK, can exit cells via an active, nonclassical secretory pathway (18, 56), displays chemotactic activity (12, 64), and is heavily posttranslationally modified by acetylation, phosphorylation, methylation, and poly(ADP-ribosylation) (6, 13, 21, 65). Whether DEK, like HMG1, fulfills the criteria of an "alarmin" (a term introduced recently to designate endogenous molecules that, if present extracellularly, signal cell and tissue damage [4]) is the subject of ongoing studies.

Concerning the intracellular function of DEK, we addressed the question of whether DEK, as a poly(ADP-ribosyl)ated protein, may be involved in DNA repair. Our results show that a knockdown of DEK expression impairs the ability of cells to resolve DNA lesions and increases sensitivity to DNA-damaging agents. Interestingly, the contribution of DEK to DNA repair becomes most evident when cells are challenged with drugs that are potent activators of PARP1, such as the topoisomerase I inhibitor camptothecin and the inducer of double-strand breaks neocarzinostatin, but not the topoisomerase II poison etoposide (7). This further strengthens the notion of a functional relationship between PARP1 and DEK in DNA repair. Further data, such as the demonstration that DEK is a substrate for PARP1 activity *in vivo* and that the two proteins share a similar distribution on open chromatin regions (see Fig. S4 in the supplemental material), suggest that DEK may be an important transducer of PAR-dependent signaling pathways even beyond the repair of damaged DNA. This sugges-

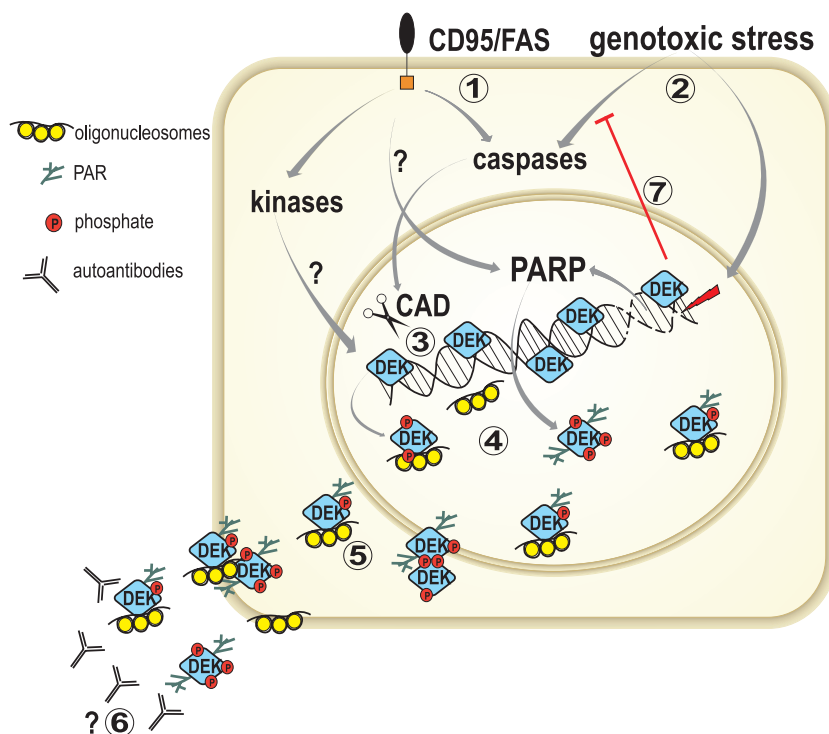


FIG. 8. Schematic model of DEK's posttranslational modifications and release in apoptosis. Induction of apoptosis either via the CD95/Fas receptor (1) or by genotoxic stress (2) results in the extracellular release of DEK. The activation of caspases and of the caspase-activated DNase (CAD) leads to fragmentation of DNA into oligonucleosomal fragments (3). PARP1 and a yet-unidentified kinase(s) are also triggered, resulting in the phosphorylation and poly(ADP)ribosylation of the protein (4). DEK leaves the nucleus both bound to oligonucleosomes and in a DNA-free form (5). Modified DEK is released into the extracellular space, where it is recognized by antibodies from JRA/JIA patients (6). In the absence of DEK, cells are more sensitive to genotoxic damage and are more prone to activate caspases (7), partly due to impaired DNA repair.

tion is corroborated by data from the literature showing that PARP1, in a manner similar to that of DEK (58), binds to (and is activated by) undamaged DNA with distorted, non-B structures, such as cruciforms, hairpins, and loops (32). Moreover, PARP1 and DEK were both found in a chromatin fraction enriched for the variant histone macroH2A (38), a marker for heterochromatin.

Finally, we observe that the degree of sensitization toward genotoxic treatment achieved by the inhibition of DEK expression is much more pronounced than the corresponding impairment of DNA repair activity, suggesting the existence of further mechanisms of DEK-dependent cytoprotection. These further mechanisms may involve the up- or downregulation of apoptosis regulatory genes, such as those encoding the anti-apoptotic proteins bcl2 (31, 41) and cIAP2 (45). A role for p53, as proposed previously (62), is unlikely, since the HeLa cell line used in this study did not reveal any change in p53 amount or activation status upon DEK knockdown (data not shown) and Jurkat cells are p53 negative.

In summary, by studying DEK in the context of cellular stress and apoptosis, this work unravels intriguing new aspects concerning both the extracellular and intracellular functions of this protein. The results point at dying cells as a so-far-unrecognized and relevant source of potentially autoantigenic DEK and at a role for DEK in the response to genotoxic damage. While our work implicates poly(ADP)ribosylation in both damage-associated aspects of DEK function, understanding

the involvement of this protein in the growing number of PAR-dependent pathways regulating genome activity under physiological conditions is a challenging question for the future.

ACKNOWLEDGMENTS

We gratefully acknowledge Damu Tang and Shigekazu Nagata for dominant negative ICAD (ICAD-dn) expression constructs, Guy G. Poirier for anti-PAR antibodies, Masano Miwa and Takashi Sugimura for 10H cells, and Henning Walczak for lz-TRAIL. We are indebted to Konstantin Matenzoglu for advice in retroviral techniques, to Caterina Giorno for apoptosis assays, and to Daniela Hermann for invaluable technical assistance.

This study was supported by grants from the German Research Foundation (DFG MA/2385 to E.F.M. and FOR 434 to A.B.) and by the Center for Junior Research Fellows of the University of Konstanz. C.S. was supported by a fellowship from the DFG Research Training Group IRTG 1331. F.K. was supported by a William D. Robinson Fellowship from the Arthritis Foundation/Michigan Chapter and is a recipient of an Arthritis Foundation Postdoctoral Fellowship. Work in the laboratory of D.M.M. is supported by grants from the National Institutes of Health and by the Burroughs Wellcome Fund Clinical Scientist Award in Translational Research. M.S.K. was supported in part by NIH training grant T32-GM07863 through the University of Michigan Medical Scientist Training Program and by a graduate research fellowship from the National Science Foundation.

REFERENCES

- Ageberg, M., U. Gullberg, and A. Lindmark. 2006. The involvement of cellular proliferation status in the expression of the human proto-oncogene DEK. *Haematologica* 91:268-269.

2. Alexiadis, V., T. Waldmann, J. Andersen, M. Mann, R. Knippers, and C. Gruss. 2000. The protein encoded by the proto-oncogene DEK changes the topology of chromatin and reduces the efficiency of DNA replication in a chromatin-specific manner. *Genes Dev.* **14**:1308–1312.
3. Bell, C. W., W. Jiang, C. F. Reich III, and D. S. Pisetsky. 2006. The extracellular release of HMGB1 during apoptotic cell death. *Am. J. Physiol. Cell Physiol.* **291**:C1318–C1325.
4. Bianchi, M. E. 2007. DAMPs, PAMPs and alarmins: all we need to know about danger. *J. Leukoc. Biol.* **81**:1–5.
5. Böhm, F., F. Kappes, I. Scholten, N. Richter, H. Matsuo, R. Knippers, and T. Waldmann. 2005. The SAF-box domain of chromatin protein DEK. *Nucleic Acids Res.* **33**:1101–1110.
6. Bonaldi, T., F. Talamo, P. Scaffidi, D. Ferrera, A. Porto, A. Bachi, A. Rubartelli, A. Agresti, and M. E. Bianchi. 2003. Monocytic cells hyperacetylate chromatin protein HMGB1 to redirect it towards secretion. *EMBO J.* **22**:5551–5560.
7. Bowman, K. J., D. R. Newell, A. H. Calvert, and N. J. Curtin. 2001. Differential effects of the poly (ADP-ribose) polymerase (PARP) inhibitor NU1025 on topoisomerase I and II inhibitor cytotoxicity in L1210 cells in vitro. *Br. J. Cancer* **84**:106–112.
8. Burkle, A. 2005. Poly(ADP-ribose). The most elaborate metabolite of NAD⁺. *FEBS J.* **272**:4576–4589.
9. Campillos, M., M. A. Garcia, F. Valdivieso, and J. Vazquez. 2003. Transcriptional activation by AP-2alpha is modulated by the oncogene DEK. *Nucleic Acids Res.* **31**:1571–1575.
10. Carro, M. S., F. M. Spiga, M. Quarto, V. Di Ninni, S. Volorio, M. Alcalay, and H. Muller. 2006. DEK Expression is controlled by E2F and deregulated in diverse tumor types. *Cell Cycle* **5**:1202–1207.
11. Cleary, J., K. V. Sitwala, M. S. Khodadoust, R. P. Kwok, N. Mor-Vaknin, M. Cebrat, P. A. Cole, and D. M. Markovitz. 2005. p300/CBP-associated factor drives DEK into interchromatin granule clusters. *J. Biol. Chem.* **280**:31760–31767.
12. Degryse, B., T. Bonaldi, P. Scaffidi, S. Muller, M. Resnati, F. Sanvito, G. Arrigoni, and M. E. Bianchi. 2001. The high mobility group (HMG) boxes of the nuclear protein HMG1 induce chemotaxis and cytoskeleton reorganization in rat smooth muscle cells. *J. Cell Biol.* **152**:1197–1206.
13. Ditsworth, D., W. X. Zong, and C. B. Thompson. 2007. Activation of poly(ADP)-ribose polymerase (PARP-1) induces release of the pro-inflammatory mediator HMGB1 from the nucleus. *J. Biol. Chem.* **282**:17845–17854.
14. Dong, X., J. Wang, F. N. Kabir, M. Shaw, A. M. Reed, L. Stein, L. E. Andrade, V. F. Trevisani, M. L. Miller, T. Fujii, M. Akizuki, L. M. Pachman, M. Satoh, and W. H. Reeves. 2000. Autoantibodies to DEK oncoprotein in human inflammatory disease. *Arthritis Rheum.* **43**:85–93.
15. Fahrer, J., R. Kranaster, M. Altmeyer, A. Marx, and A. Burkle. 2007. Quantitative analysis of the binding affinity of poly(ADP-ribose) to specific binding proteins as a function of chain length. *Nucleic Acids Res.* **35**:e143.
16. Faulkner, N. E., J. M. Hilfinger, and D. M. Markovitz. 2001. Protein phosphatase 2A activates the HIV-2 promoter through enhancer elements that include the pets site. *J. Biol. Chem.* **276**:25804–25812.
17. Gamble, M. J., and R. P. Fisher. 2007. SET and PARP1 remove DEK from chromatin to permit access by the transcription machinery. *Nat. Struct. Mol. Biol.* **14**:548–555.
18. Gardella, S., C. Andrei, D. Ferrera, L. V. Lotti, M. R. Torrisi, M. E. Bianchi, and A. Rubartelli. 2002. The nuclear protein HMGB1 is secreted by monocytes via a non-classical, vesicle-mediated secretory pathway. *EMBO Rep.* **3**:995–1001.
19. Grottko, C., K. Mantwill, M. Dietel, D. Schadendorf, and H. Lage. 2000. Identification of differentially expressed genes in human melanoma cells with acquired resistance to various antineoplastic drugs. *Int. J. Cancer* **88**:535–546.
20. Hollenbach, A. D., C. J. McPherson, E. J. Mientjes, R. Iyengar, and G. Grosveld. 2002. Daxx and histone deacetylase II associate with chromatin through an interaction with core histones and the chromatin-associated protein Dek. *J. Cell Sci.* **115**:3319–3330.
21. Ito, I., J. Fukazawa, and M. Yoshida. 2007. Post-translational methylation of high mobility group box 1 (HMGB1) causes its cytoplasmic localization in neutrophils. *J. Biol. Chem.* **282**:16336–16344.
22. Jiang, W., C. W. Bell, and D. S. Pisetsky. 2007. The relationship between apoptosis and high-mobility group protein 1 release from murine macrophages stimulated with lipopolysaccharide or polyinosinic-polycytidylic acid. *J. Immunol.* **178**:6495–6503.
23. Kappes, F., K. Burger, M. Baack, F. O. Fackelmayer, and C. Gruss. 2001. Subcellular localization of the human proto-oncogene protein DEK. *J. Biol. Chem.* **276**:26317–26323.
24. Kappes, F., C. Damoc, R. Knippers, M. Przybylski, L. A. Pinna, and C. Gruss. 2004. Phosphorylation by protein kinase CK2 changes the DNA binding properties of the human chromatin protein DEK. *Mol. Cell. Biol.* **24**:6011–6020.
25. Kappes, F., I. Scholten, N. Richter, C. Gruss, and T. Waldmann. 2004. Functional domains of the ubiquitous chromatin protein DEK. *Mol. Cell. Biol.* **24**:6000–6010.
26. Kawamitsu, H., H. Hoshino, H. Okada, M. Miwa, H. Momoi, and T. Sugimura. 1984. Monoclonal antibodies to poly(adenosine diphosphate ribose) recognize different structures. *Biochemistry* **23**:3771–3777.
27. Ko, S. I., I. S. Lee, J. Y. Kim, S. M. Kim, D. W. Kim, K. S. Lee, K. M. Woo, J. H. Baek, J. K. Choo, and S. B. Seo. 2006. Regulation of histone acetyltransferase activity of p300 and PCAF by proto-oncogene protein DEK. *FEBS Lett.* **580**:3217–3222.
28. Kondoh, N., T. Wakatsuki, A. Ryo, A. Hada, T. Aihara, S. Horiuchi, N. Goseki, O. Matsubara, K. Takenaka, M. Shichita, K. Tanaka, M. Shuda, and M. Yamamoto. 1999. Identification and characterization of genes associated with human hepatocellular carcinogenesis. *Cancer Res.* **59**:4990–4996.
29. Kramer, P. H. 2000. CD95's deadly mission in the immune system. *Nature* **407**:789–795.
30. Kroes, R. A., A. Jastrow, M. G. McLone, H. Yamamoto, P. Colley, D. S. Kersey, V. W. Yong, E. Mkrdichian, L. Cerullo, J. Leestma, and J. R. Moskal. 2000. The identification of novel therapeutic targets for the treatment of malignant brain tumors. *Cancer Lett.* **156**:191–198.
31. Lee, K. S., D. W. Kim, J. Y. Kim, J. K. Choo, K. Yu, and S. B. Seo. 2007. Caspase-dependent apoptosis induction by targeted expression of DEK in drosophila involves histone acetylation inhibition. *J. Cell. Biochem.* **103**:1283–1293.
32. Lonskaya, I., V. N. Potaman, L. S. Shlyakhtenko, E. A. Oussatcheva, Y. L. Lyubchenko, and V. A. Soldatenkov. 2005. Regulation of poly(ADP-ribose) polymerase-1 by DNA structure-specific binding. *J. Biol. Chem.* **280**:17076–17083.
33. McGarvey, T., E. Rosonina, S. McCracken, Q. Li, R. Arnaut, E. Mientjes, J. A. Nickerson, D. Awrey, J. Greenblatt, G. Grosveld, and B. J. Blencowe. 2000. The acute myeloid leukemia-associated protein, DEK, forms a splicing-dependent interaction with exon-product complexes. *J. Cell Biol.* **150**:309–320.
34. Mendoza-Alvarez, H., and R. Alvarez-Gonzalez. 2001. Regulation of p53 sequence-specific DNA-binding by covalent poly(ADP-ribosylation). *J. Biol. Chem.* **276**:36425–36430.
35. Mor-Vaknin, N., A. Punturieri, K. Sitwala, N. Faulkner, M. Legendre, M. S. Khodadoust, F. Kappes, J. H. Ruth, A. Koch, D. Glass, L. Petruzzelli, B. S. Adams, and D. M. Markovitz. 2006. The DEK nuclear autoantigen is a secreted chemotactic factor. *Mol. Cell. Biol.* **26**:9484–9496.
36. Ohtsuki, K., and N. Ishida. 1975. Neocarzinostatin-induced breakdown of deoxyribonucleic acid in HeLa-S3 cells. *J. Antibiot. (Tokyo)* **28**:143–148.
37. Orlic, M., C. E. Spencer, L. Wang, and B. L. Gallie. 2006. Expression analysis of 6p22 genomic gain in retinoblastoma. *Genes Chromosomes Cancer* **45**:72–82.
38. Ouararhni, K., R. Hadj-Slimane, S. Ait-Si-Ali, P. Robin, F. Miettinen, A. Harel-Bellan, S. Dimitrov, and A. Hamiche. 2006. The histone variant mH2A1.1 interferes with transcription by down-regulating PARP-1 enzymatic activity. *Genes Dev.* **20**:3324–3336.
39. Pagano, M. A., M. Andrzejewska, M. Ruzzene, S. Sarno, L. Cesaro, J. Bain, M. Elliott, F. Meggio, Z. Kazimierzczuk, and L. A. Pinna. 2004. Optimization of protein kinase CK2 inhibitors derived from 4,5,6,7-tetrabromobenzimidazole. *J. Med. Chem.* **47**:6239–6247.
40. Pleschke, J. M., H. E. Kleczkowska, M. Strohm, and F. R. Althaus. 2000. Poly(ADP-ribose) binds to specific domains in DNA damage checkpoint proteins. *J. Biol. Chem.* **275**:40974–40980.
41. Reed, J. C. 2006. Proapoptotic multidomain Bcl-2/Bax-family proteins: mechanisms, physiological roles, and therapeutic opportunities. *Cell Death Differ.* **13**:1378–1386.
42. Rensing-Ehl, A., K. Frei, R. Flury, B. Matiba, S. M. Mariani, M. Weller, P. Aebischer, P. H. Kramer, and A. Fontana. 1995. Local Fas/APO-1 (CD95) ligand-mediated tumor cell killing in vivo. *Eur. J. Immunol.* **25**:2253–2258.
43. Sakahira, H., M. Enari, and S. Nagata. 1998. Cleavage of CAD inhibitor in CAD activation and DNA degradation during apoptosis. *Nature* **391**:96–99.
44. Sakahira, H., M. Enari, Y. Ohsawa, Y. Uchiyama, and S. Nagata. 1999. Apoptotic nuclear morphological change without DNA fragmentation. *Curr. Biol.* **9**:543–546.
45. Sammons, M., S. S. Wan, N. L. Vogel, E. J. Mientjes, G. Grosveld, and B. P. Ashburner. 2006. Negative regulation of the RelA/p65 transactivation function by the product of the DEK proto-oncogene. *J. Biol. Chem.* **281**:26802–26812.
46. Scaffidi, P., T. Misteli, and M. E. Bianchi. 2002. Release of chromatin protein HMGB1 by necrotic cells triggers inflammation. *Nature* **418**:191–195.
47. Schreiber, V., F. Dantzer, J. C. Ame, and G. de Murcia. 2006. Poly(ADP-ribose): novel functions for an old molecule. *Nat. Rev. Mol. Cell. Biol.* **7**:517–528.
48. Simbulan-Rosenthal, C. M., D. S. Rosenthal, S. Iyer, A. H. Boulares, and M. E. Smulson. 1998. Transient poly(ADP-ribosylation) of nuclear proteins and role of poly(ADP-ribose) polymerase in the early stages of apoptosis. *J. Biol. Chem.* **273**:13703–13712.
49. Sitwala, K. V., K. Adams, and D. M. Markovitz. 2002. YY1 and NF-Y binding sites regulate the transcriptional activity of the dek and dek-can promoter. *Oncogene* **21**:8862–8870.
50. Sitwala, K. V., N. Mor-Vaknin, and D. M. Markovitz. 2003. Minireview:

- DEK and gene regulation, oncogenesis and AIDS. *Anticancer Res.* **23**:2155–2158.
51. Soares, L. M., K. Zanier, C. Mackereth, M. Sattler, and J. Valcarcel. 2006. Intron removal requires proofreading of U2AF/3' splice site recognition by DEK. *Science* **312**:1961–1965.
 52. Suzuki, Y., Y. Ono, and Y. Hirabayashi. 1998. Rapid and specific reactive oxygen species generation via NADPH oxidase activation during Fas-mediated apoptosis. *FEBS Lett.* **425**:209–212.
 53. Tabbert, A., F. Kappes, J. Kellermann, F. Lottspeich, and E. Ferrando-May. 2006. Hypophosphorylation of the architectural chromatin protein DEK in death-receptor induced apoptosis revealed by the isotope coded protein label proteomic platform. *Proteomics* **6**:5758–5772.
 54. Takahashi, A., and T. Ohnishi. 2005. Does gammaH2AX foci formation depend on the presence of DNA double strand breaks? *Cancer Lett.* **229**:171–179.
 55. von Lindern, M., M. Fornerod, S. van Baal, M. Jaegle, T. de Wit, A. Buijs, and G. Grosveld. 1992. The translocation (6;9), associated with a specific subtype of acute myeloid leukemia, results in the fusion of two genes, *dek* and *can*, and the expression of a chimeric, leukemia-specific *dek-can* mRNA. *Mol. Cell. Biol.* **12**:1687–1697.
 56. Wähämaa, H., T. Vällerskog, S. Qin, C. Lunderius, G. LaRosa, U. Andersson, and H. E. Harris. 2007. HMGB1-secreting capacity of multiple cell lineages revealed by a novel HMGB1 ELISPOT assay. *J. Leukoc. Biol.* **81**:129–136.
 57. Walczak, H., R. E. Miller, K. Ariail, B. Gliniak, T. S. Griffith, M. Kubin, W. Chin, J. Jones, A. Woodward, T. Le, C. Smith, P. Smolak, R. G. Goodwin, C. T. Rauch, J. C. Schuh, and D. H. Lynch. 1999. Tumoricidal activity of tumor necrosis factor-related apoptosis-inducing ligand in vivo. *Nat. Med.* **5**:157–163.
 58. Waldmann, T., M. Baack, N. Richter, and C. Gruss. 2003. Structure-specific binding of the proto-oncogene protein DEK to DNA. *Nucleic Acids Res.* **31**:7003–7010.
 59. Waldmann, T., C. Eckerich, M. Baack, and C. Gruss. 2002. The ubiquitous chromatin protein DEK alters the structure of DNA by introducing positive supercoils. *J. Biol. Chem.* **277**:24988–24994.
 60. Waldmann, T., I. Scholten, F. Kappes, H. G. Hu, and R. Knippers. 2004. The DEK protein—an abundant and ubiquitous constituent of mammalian chromatin. *Gene* **343**:1–9.
 61. Wessel, D., and U. I. Flugge. 1984. A method for the quantitative recovery of protein in dilute solution in the presence of detergents and lipids. *Anal. Biochem.* **138**:141–143.
 62. Wise-Draper, T. M., H. V. Allen, E. E. Jones, K. B. Habash, H. Matsuo, and S. I. Wells. 2006. Apoptosis inhibition by the human DEK oncoprotein involves interference with p53 functions. *Mol. Cell. Biol.* **26**:7506–7519.
 63. Wise-Draper, T. M., H. V. Allen, M. N. Thobe, E. E. Jones, K. B. Habash, K. Munger, and S. I. Wells. 2005. The human DEK proto-oncogene is a senescence inhibitor and an upregulated target of high-risk human papillomavirus E7. *J. Virol.* **79**:14309–14317.
 64. Yang, D., Q. Chen, H. Yang, K. J. Tracey, M. Bustin, and J. J. Oppenheim. 2007. High mobility group box-1 protein induces the migration and activation of human dendritic cells and acts as an alarmin. *J. Leukoc. Biol.* **81**:59–66.
 65. Youn, J. H., and J. S. Shin. 2006. Nucleocytoplasmic shuttling of HMGB1 is regulated by phosphorylation that redirects it toward secretion. *J. Immunol.* **177**:7889–7897.